

L. KUCHARIKOVÁ<sup>\*#</sup>, E. TILLOVÁ<sup>\*</sup>, M.S. BONEK<sup>\*\*</sup>, M. CHALUPOVÁ<sup>\*</sup>

## USING DEEP ETCHING IN THE STUDY OF EUTECTIC SILICON 3D-MORPHOLOGY IN AISi7MgTi CAST ALLOY

The effect of combination grain refinement with AlTi5B1 master (55 ppm) and Sr-modification with AlSr5 master (20, 30, 40, 50 and 60 ppm) on the microstructure, tensile and hardness properties of AlSi7MgTi cast alloy were systematically investigated. Eutectic silicon was studied by optical and scanning electron microscopy after standard (0.5% HF) and deep etching (HCl). Morphology of eutectic Si changes from compact plate-like (as-cast state) to fibbers (after modification). Si-fibbers in samples with 50 and 60 ppm Sr coarsen probably as a result of over-modification. The optimum mechanical properties has the experimental material which was grain refined and modified with 40 ppm of Sr (UTS = 220.6 MPa; ductility = 6.1%, and 82.3 HBW 5/250/15).

*Keywords:* modification, refinement, eutectic Si morphology, deep etching

### 1. Introduction

The aluminium cast alloys have excellent physical and mechanical properties for a number of industry applications. The automotive casts are made especially from Al-Si cast alloys thanks to their weight and properties. These materials were divided into three groups: hypo-eutectic with a Si concentration from 4 to 10 wt. %, eutectic with a Si concentration from 10 to 13 wt. %, and hyper-eutectic with a Si concentration up to 26 wt. % [1-2]. Paramount application of Al-Si cast alloys are hypo-eutectic or near-eutectic ternary alloys Al-Si-Mg and Al-Si-Cu [1,3,4]. These materials have excellent castability, good corrosion and wear resistance, high strength stiffness to weight ratio (good mechanical properties), low density and thermal expansion, high productivity and low shrinkage rate, recycling possibilities, and low cost. Also can be given a wide variety of surface finishes and it can be cast and produced into almost any form of a product [4]. Hypo-eutectic and near-eutectic Al-Si-Mg alloys, which have been usually used to produce castings, have higher strength and rigidity [5]. One of the few disadvantages is their morphology of eutectic (the mechanical mixture of eutectic Si particles and Al-matrix), which is characterized by plate-like shaped (lamellar, coarse-grained) silicone that has a detrimental effect on the mechanical properties of these materials (especially decreases elongation and ductility) [6,7]. The eutectic Si morphology changes cause either chemical modification (addition of trace levels of certain additive – modifier to a molten Al-Si) or cooling rate during casting, and the heat treatment and so on after casting. These technological processes lead to changes

morphology of eutectic Si from coarse plate-like (lamellar) to fibrous, fine fibrous and spherical [8-12].

The process of modification has been used since the end of the 19<sup>th</sup> century to improve the aluminium alloys. Nowadays, the operations of modification (using various techniques) are applicable to most of the commercial alloys [4]. Common modifiers are e.g. Na, Sr, Sb, the other modifiers which effect was investigated are Ba, P, Ca, Er, Eu, Li, Y, Ce and so on in aluminium cast alloys [10,13,14]. Natrium (Na) was the modifier first used in the foundries. Its application is difficult because it has low solubility in molten aluminium, a high vapour pressure, and is also rapidly lost to oxidation after addition. Very low Na concentrations of 0.005 to 0.015% are required for effective modification [15,16]. Standard industry practice has a range of 0.015 to 0.05% [17,18]. Besides Na begins the Sr used as a modifier. Strontium (Sr) is easily added via master alloys with nearly 100% recovery and its loss to oxidation is slow [15]. Approximately 0.02 wt. % of Sr addition will refine platelets Si morphology into a fibrous form, but has no effect on the deposition of primary Al-dendrite [17]. The advantages of Sr modification are to improve the ductility, fracture and impact properties, and can also be effectively used to reduce the solution treatment time of the alloy. The disadvantages are the apparent increase in porosity in the casting [7]. The modification with Sb leads to reducing the susceptibility to gassing, thereby producing very solid castings. Even the treatment with Sb is not dependent on such processing variables as holding time, remelting, and degassing as by modification with Na and Sr additions. In this case, the modified structure differs; a more acicular refined

\* UNIVERSITY OF ŽILINA, FACULTY OF MECHANICAL ENGINEERING, UNIVERZITNÁ 8215/1, 010 26 ŽILINA, SLOVAK REPUBLIC

\*\* SILESIAN UNIVERSITY OF TECHNOLOGY, INSTITUTE OF ENGINEERING MATERIALS AND BIOMATERIALS, 18A KONARSKIEGO STR., 44 100 GLIWICE, POLAND

# Corresponding author: lenka.kucharikova@fstroj.uniza.sk

eutectic is obtained compared to the uniform lace-like dispersed structures of Na, Ca, or Sr modified metal. The disadvantage of Sb: is not compatible with other modifying elements. If Sb and other modifiers are present, coarse Sb-containing intermetallic is formed that preclude the attainment of an effectively modified structure and adversely affect casting results [16,18,19]. To be effective in modification, Sb must be allowed to approximately 0.06%. In practice, Sb is employed in the much higher range of 0.10 to 0.50% [16].

The change of the Si morphology with Li modification is mostly depending on to cooling rate [11]. Li was found to be effective in modifying the  $\beta$ -Al<sub>5</sub>FeSi intermetallic compound and plate-like eutectic Si into fine and independent ones. However, the Li containing alloys are prone to casting defects such as porosity [20]. The studies have revealed the potential of Ca to modify the eutectic silicon, altering the morphology of the Fe-rich intermetallic to less harmful shapes and improving the fracture toughness and impact properties of high iron containing Al-Si, Al-Si-Cu, and Al-Si-Mg casting alloys [21]. P is the most effective modifier of primary Si in hypereutectic Al-Si alloy and has no modification effect on the eutectic Si, the eutectic Si can still keep the large plate-like (needle) shape [22]. P reacts with Na and probably with Sr and Ca to form phosphides that nullify the intended modification additions. It is therefore desirable to use low-phosphorous metal when modification may be used. The allowed amount of P in primary ingots is less than 5 ppm [16].

In some materials, modification of the shape and size of Si particles together with grain refinement in the Al-matrix is key to improve the mechanical properties [4,12,14,17,23]. The main refiners in aluminium alloys are Ti, B and their combination. In recent years the usage of Y, Yr and V as grain refiners were studied, too [14,24]. Ti is the element with the highest growth restriction factor, which plays an important role in the grain refinement of Al by means heterogeneous nucleation. A lot of scientific work shows that the AlB<sub>3</sub> master alloy performs very well in Al-Si cast alloys, but if these alloys contain Ti impurity in a percentage greater than 0.04 wt. % the AlB<sub>3</sub> master alloy grain refining potency is equal to that of commercial master alloys based on Al-Ti-B ternary system (i.e. AlTi<sub>5</sub>B<sub>1</sub> and AlTi<sub>3</sub>B<sub>3</sub> [25].

Therefore, the main objective of this work was using of deep etching to study the optimal amount of Sr modification in AlSi<sub>7</sub>MgTi alloy required for the best mechanical properties.

## 2. Experimental procedure

The experimental material (AlSi<sub>7</sub>MgTi cast alloy) was received in the form of samples for mechanical tests (tensile tests) from company FIMES, a.s., Czech Republic. The chemical analysis of commercial ingots of primary alloy (without modification and grain refinement) was carried out using an arc spark spectroscopy at the University of Žilina (Table 1).

Experimental alloy (commercial ingots of primary alloy) was molten in a graphitic

crucible coated with a protective coating in a resistance oven. The temperature of molten metal was stabilized at  $735 \pm 5^\circ\text{C}$  for grain refinement of experimental material. Refiner was added to the melt in the form of AlTi<sub>5</sub>B<sub>1</sub> master in amount of 55 ppm. Sr-addition was achieved by introducing different amounts of an AlSr<sub>5</sub> master alloy. AlSr<sub>5</sub> master alloy was added to the unmodified alloy in such quantities that the Sr content was 20, 30, 40, 50 and 60 ppm. The temperature of modification was  $730 \pm 5^\circ\text{C}$ . Refinement and modification was realized with immersion bell for holding time 3 minutes. Before casting of the experimental samples, the melt was refined with AlCu<sub>4</sub>B<sub>6</sub> salt at  $740 \pm 5^\circ\text{C}$ . The experimental samples were cast with method of precise casting to a removable model into the shell forms. The forms were heated on  $440 \pm 5^\circ\text{C}$ . After the casting, 12 cylindrical cast specimens with the 20 mm diameter and 200 mm length were obtained for each Sr-amount.

AlSi<sub>7</sub>MgTi cast alloy has good corrosion resistance and mechanical properties, good castability and machinability, adequate polishability. These materials are used for thin-walled castings for the automotive and aerospace industry [26].

Cast testing specimens were subjected for the mechanical tests: tensile test, and hardness test. Mechanical properties were measured according to the following standards: STN EN ISO 6892-1, and STN EN ISO 6506-1. Hardness measurement for experimental alloy was performed on polished samples by using Brinell hardness tester with a load of 250 kp (1 kp = 9.80665 N), the testing ball with 5 mm in diameter and a dwell time of 15s (mark is: HBW 5/250/15). Ultimate tensile strength was measured using ZDM 30 testing machine (with nominal energy 0-30 kN). The dimensions of testing specimens were: the cross section  $\varnothing$  10 mm and initial measured length of 50 mm. The resulting Brinell hardness value and ultimate tensile strength value are arithmetic mean of six separate measurements. All the tests were performed at an ambient temperature ( $\sim 22^\circ\text{C}$ ).

The samples for the change of morphology observation were prepared from selected tensile specimens (after testing) and the microstructures were studied using an optical microscope Neophot 32 and scanning electron microscope VEGA LMU II. Samples for optical microscope were prepared by standard metallographic procedures (wet ground on SiC papers, DP polished with 3  $\mu\text{m}$  m diamond pastes followed by Struers Op-S and etched for study at an optical microscope by etchant reagents 0.5% HF and MA). Molybdenum ammonia (MA) was used for highlighting intermetallic phases in the microstructure. Samples for observation in scanning electron microscope were standardly etched by 0.5% HF (; deep etched for 30 s in HCl solution (36 ml HCl, 100 ml distilled water) in order to reveal the three-dimensional morphology of the phases (eutectic silicon or intermetallic phases) [2]. Thereafter the samples were washed

TABLE 1  
Chemical analysis of commercial ingots from the AlSi<sub>7</sub>MgTi alloys, in wt. %

Si	Mg	Ti	Cu	Mn	Fe	Zn	Ni	Sr	Ca	P	Al
6.9	0.29	0.123	0.001	0.05	0.11	0.001	0.004	0.05	0.002	0.0001	balance

subsequently with ethanol and dried. Specimens for SEM observation were also deep-etched from 20 to 50 s in HCl solution in order to reveal the three-dimensional morphology of the silicon phase. The specimen preparation procedure for deep-etching consists of dissolving the aluminium matrix in a reagent that will not attack the eutectic components or intermetallic phases. The residuals of the etching products should be removed by intensive rinsing in alcohol. The preliminary preparation of the specimen is not necessary, but removing the superficial deformed or contaminated layer can shorten the process. Using prepared samples, a three-dimensional morphology was observed once it was scanned by the VEGA LMU II electron microscope.

### 3. Results and discussion

#### 3.1. Mechanical properties

Early stages of aluminium cast alloy damage are typically dominated by the fracture of Si particles in aluminium alloys and are mostly attributed to the high local stress-concentration (plate-like, or lamellar morphology). The fatigue properties, fatigue crack initiation and propagation, wear resistance, mechanical properties are influenced by the morphology of Si particles, and is therefore important to change their shape [27-32].

The experimental material has in a cast state (without grain refinement and modification) ultimate tensile strength (UTS) 186.5 MPa, the ductility 3.16 % and Brinell hardness 61.4 HBW 5/250/15. Mechanical properties were changed as a result of grain refinement and modification (20-60 ppm) of the experimental alloy. The results are shown in Fig. 1.

The results of ductility and ultimate tensile strength shows that with increasing of Sr amount increase their value up to 40 ppm of Sr compared to as-cast state. But 60 ppm of Sr lead to decreasing their value (Fig. 1).

The Brinell hardness increases up to 30 ppm of Sr, at 40 ppm little decreases, but state at 60 ppm decrease its value comparable to as-cast state (Fig. 1). The optimum properties for experimental 10 material were reached after modification with 40 ppm of Sr. The UTS was about 5% higher (220.6 MPa), ductility was about 20.16% higher (6.1%), and HBW was about

29% higher (82.3 HBW 5/250/15) comparison to as-cast state. These results are corresponding with changes in morphology of eutectic Si particles (Fig. 4 and 5).

#### 3.2. Microstructure

The typical microstructure of AlSi7MgTi cast alloy consists of the  $\alpha$ -matrix, eutectic Si particles, Fe and Mg-rich intermetallics. In the alloy used for experiments two main Fe-rich intermetallic phases have been observed: the  $\alpha$ -Al<sub>15</sub>(FeMn)<sub>3</sub>Si<sub>2</sub> with Chinese script and cubic crystal structure and the  $\beta$ -Al<sub>5</sub>FeSi having a needle-like appearance and monoclinic crystal structure (Fig. 2).

Long Al<sub>5</sub>FeSi needles are brittle and appear as highly faceted platelets, which causes the loss of strength and ductility in the cast alloy. Intermetallic phases on base Mg was observed as grouped thin particles. Eutectic Si was observed in form of needles in as-cast state. In modifier samples (e.g. 20 ppm Sr) the undissolved modifier AlSr5 in form spherical shape was observed (Fig. 2b,c).

#### 3.3. Morphology of eutectic Si

Grain refinement and modification using small additions of Al-Ti-B or Al-Ti-C (as refiners) and AlSr master alloys (as modifiers) are the commonly used method for controlling the microstructures of aluminium alloys [12,17,22,33,34]. Grain refinement primarily reduces the grain size, change SDAS factor, minimization of porosity, reduced chemical segregation, and yet modification alters the morphology of the eutectic Si from a plate-like to a fibrous morphology (Fig. 3).

Strontium is the most widely used and a very effective element for modifying the morphology of eutectic silicon. Fig. 4 shows the Si- morphology evolution after Sr-modification. In as-cast state has eutectic silicon plate-like (in cut-line needle-like) morphology (Fig. 4a) with the needle-length of 20-50  $\mu$ m and width of 2-5  $\mu$ m. For the modified alloy (as shown in Fig. 4b-f) needle/plate-like eutectic silicon changed into particles, illustrating that Sr-modification is an effective way for eutectic silicon modification. In samples with 20, 30 and 40 ppm of Sr, eutectic silicon is observed

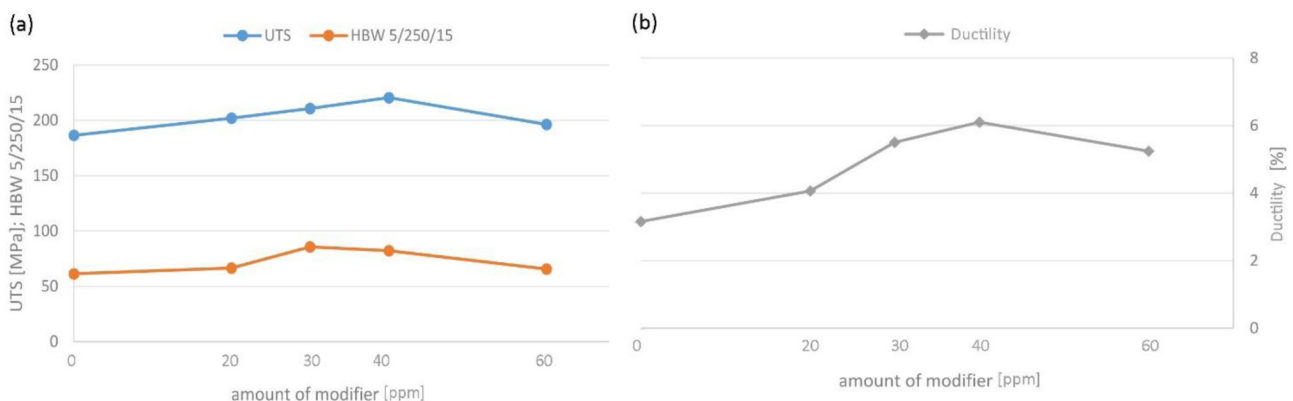


Fig. 1. Effect of modification onto mechanical properties of AlSi7MgTi alloy

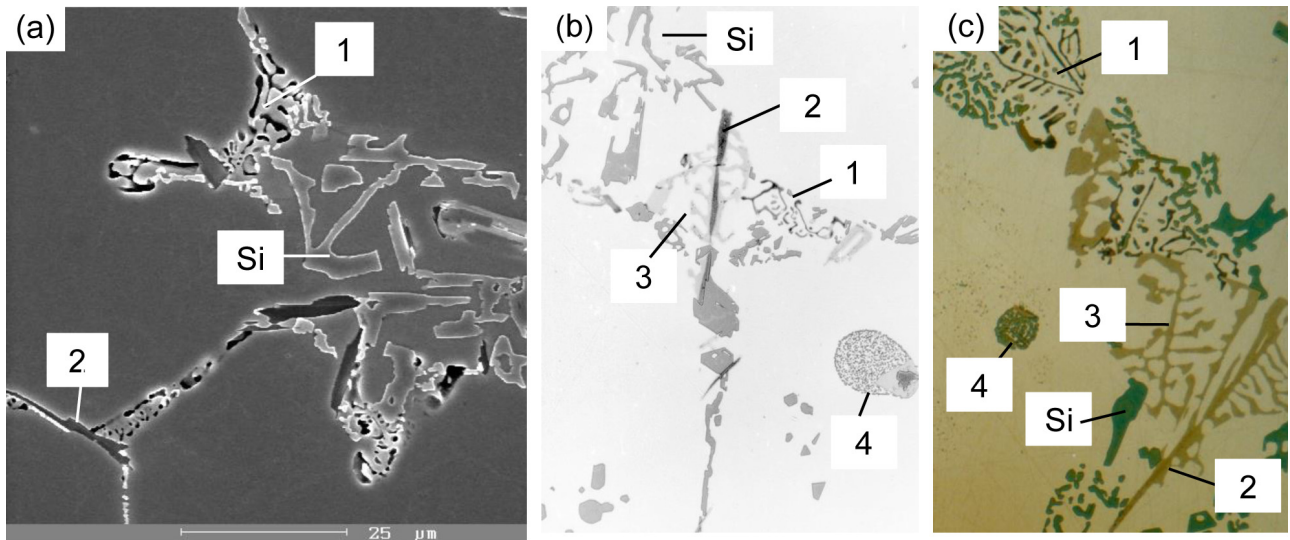


Fig. 2. Microstructure of experimental material – detail of intermetallic phases: (a) SEM micrograph of as-state state, etch. 0.5 % HF; (b) 20 ppm Sr, etch. 0.5 % HF; (c) 20 ppm Sr, etch. MA; 1 –  $Mg_2Si$ ; 2 –  $Al_5FeSi$ ; 3 –  $Al_{15}(FeMn)_3Si_2$ ; 4 –  $AlSr_5$ ;



Fig. 3. Schematically model of effect of technological processes on structural features in aluminium alloys [37,38]; (a) refiners effect onto Al-matrix; (b) modifiers effect onto eutectic Si particles

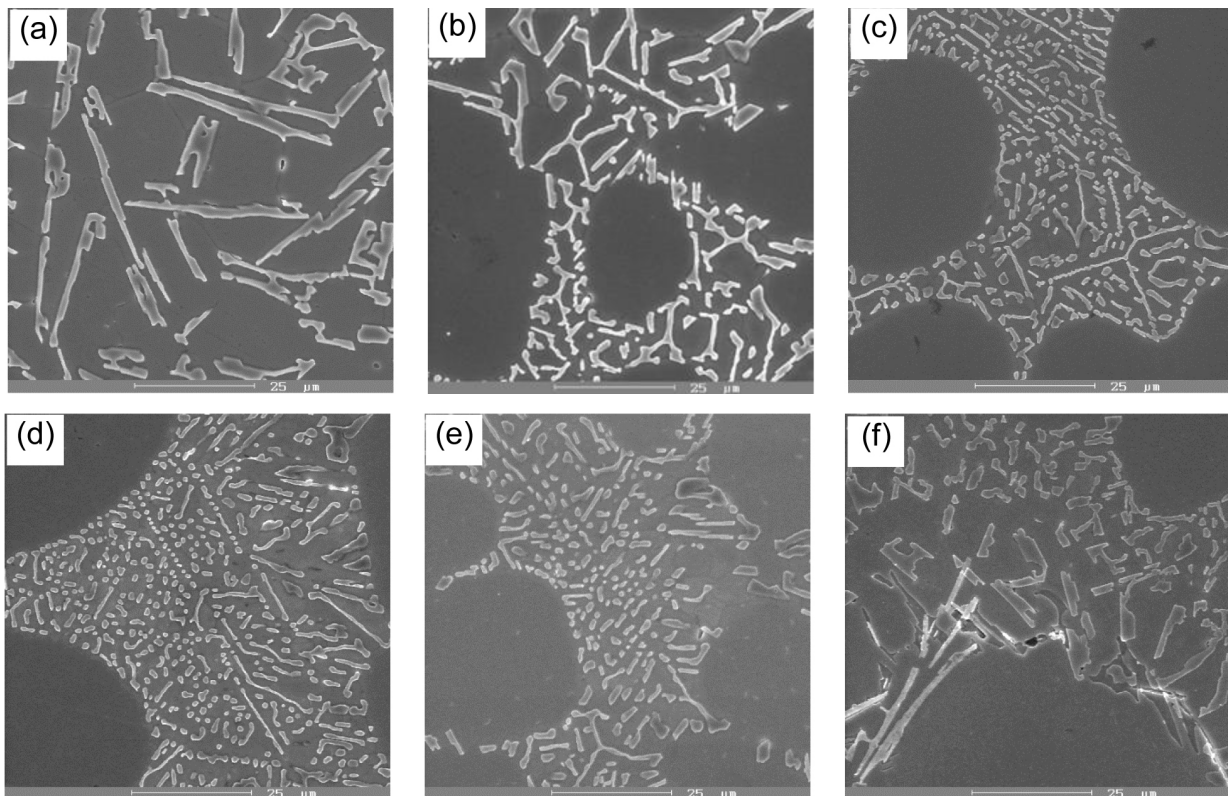


Fig. 4. SEM microstructures with various Sr content, etch. 0.5 % HF: (a) as-cast state; (b) 20 ppm; (c) 30 ppm; (d) 40 ppm; (e) 50 ppm; (f) 60 ppm

as fine round particles (Fig. 4b-d) with the length of 1-5  $\mu\text{m}$ . The fully modified Si was obtained in samples modified with 40 ppm Sr and therefore the mechanical properties were the highest (Fig. 4d, Fig. 1). Samples with 50 or 60 ppm of Sr we can be marked as over modified, eutectic silicon gradually coarsen (Fig. 4e,f).

In consideration of the modification mechanism, two hypotheses have been proposed and popularly accepted. One is the impurity induced twinning (IIT) theory proposed by Lu and Hellawell [35] that Si can be poisoned by the modifier and promoting twinning. Another modification mechanism is the twin plane re-entrant edge (TPRE) mechanism and it suggested that the re-entrant edges can provide the sites for Si growth in the  $\langle 211 \rangle$  direction. Meanwhile, it's believed that modifier will poison the re-entrant of the twin grooves and finally change the morphology of eutectic Si [36]. Fig. 5 shows the comparison of the 3D- morphology of eutectic silicon observed by SEM on the deep-etched samples. Fig. 5a documented the eutectic silicon in the as-cast state. The silicon phase exhibits a typical coarse plate-like form. Most likely these silicon plates grew epitaxially from the surrounding primary aluminium dendrites. With the Sr addition, eutectic Si crystals become significantly refined from long plates to fine fibbers. Fibbers grow as clusters from a single nucleating site (Fig. 5b-f). The smallest amount of modifier (20 ppm) is insufficient to complete change from plate-like to fibrous morphology (Fig. 5b). With increasing of modifier up to 40 ppm Sr are almost all plate-like eutectic Si particles changed to fine fibber and other fibbers are rounded with a round cross-section. The higher amount of modifier (above 40 ppm) leads to negatively effect. Fibbers corresponds with metallographic

sections, i.e. bunched in the middle of the arrangement prevailing fine round fibbers and outwards, increased incidence of so called plate-like type with typical hexagonal shape (Fig. 5e,f).

These Si-morphological changes are directly proportional to the mechanical properties of the experimental material. The optimum morphology changes of Si particles are at 40 ppm of Sr in microstructure of experimental material (AlSi7MgTi cast alloy). The Si particles were obtained in small, spherical and evenly distributed shape which according to authors [27-32] lead to optimum tensile, but also better impact and fatigue properties of experimental alloys can be obtained.

#### 4. Conclusion

The present study describes the effect of Sr- modification (20-60 ppm) on morphology changes of eutectic Si particles in AlSi7MgTi cast alloy. For a more detailed study of the 3D- morphology of the Si phases it is appropriate to apply deep etching. Based on the results obtained, the conclusions can be summarized as follows:

- Microstructure of experimental alloy consists of Al-matrix, eutectic and intermetallic phases:  $\text{Mg}_2\text{Si}$ ,  $\text{Al}_5\text{FeSi}$  and  $\text{Al}_{15}(\text{FeMg})_3\text{Si}_2$ .
- The additions of AlSr5 master modify the eutectic Si from plate-like (needle) to fibrous (rounded fibbers). The optimal Sr content was 40 ppm, leading to the utility tensile strength, elongation and hardness improved by 5%, 20.16% and 29% compared with the as-cast state.

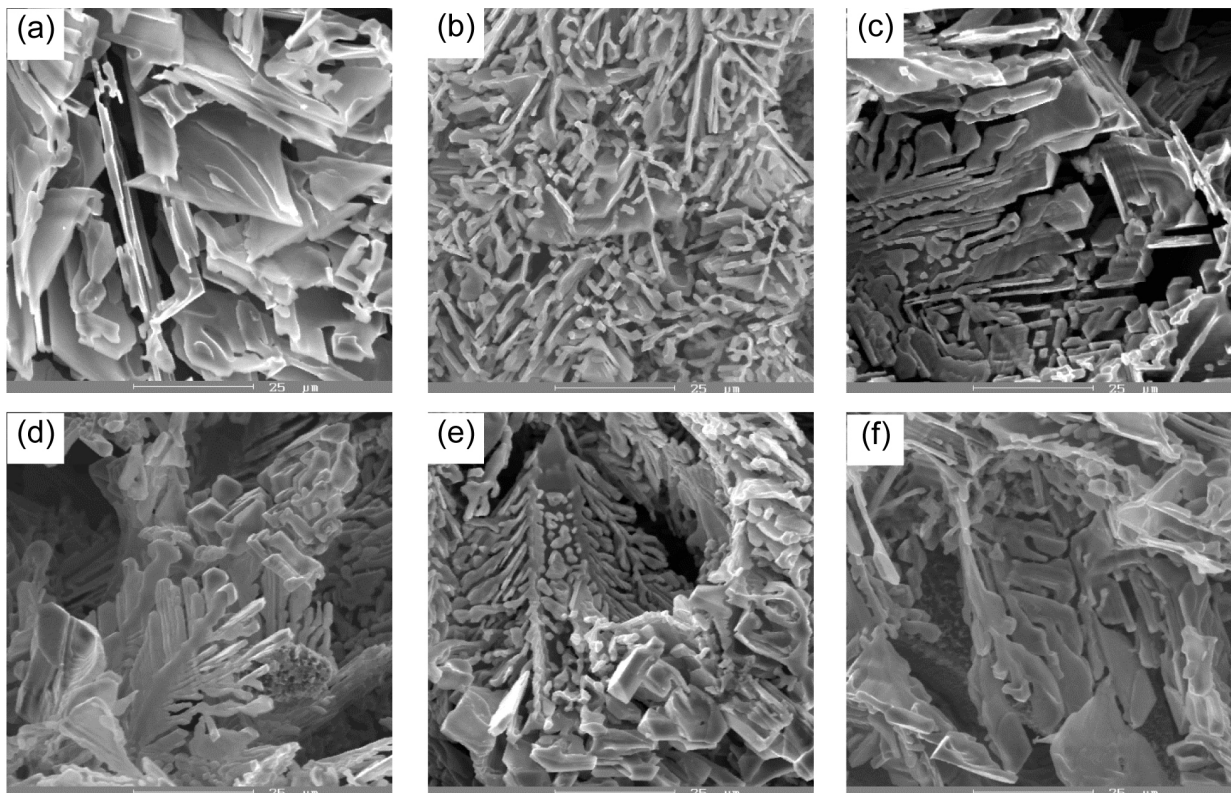


Fig. 5. Deep etched SEM micrographs of samples contain Sr: (a) as-cast state; (b) 20 ppm; (c) 30 ppm; (d) 40 ppm; (e) 50 ppm; (f) 60 ppm

### Acknowledgement

This work would not have been possible without the constant support from the Scientific Grant Agency of the Ministry of Education, Science and Sports of the Slovak Republic and Slovak Academy of Sciences, N° 1/0533/15. The authors would also like to extend their sincere thanks to Mrs. Anna Macúchová for the preparation of metallographic samples.

Publication supported as a part of the Rector's grant in the area of scientific research and development works. Silesian University of Technology, Poland 10/010/RGJ18/0200.

### REFERENCES

- [1] T. Tański, K. Labisz, B. Krupińska, M. Krupiński, M. Król, R. Maniara, W. Borek, J. Therm. Anal. Calorim. **123**/1, 63-74 (2016). DOI 10.1007/s10973-015-4871-y.
- [2] M. Michna, et al. Aluminium materials and technologies from A to Z. Adin s.r.o Prešov, (2007).
- [3] N. Náprstková, J. Cais, Production Engineering Archives **3**/2, 10-13 (2014).
- [4] A. Bialobrzeski, Archives of Foundry Engineering **7**/1, 53-56 (2007).
- [5] Y. Wang, H. Liao, Y. Wu, J. Yang, Materials and Design **53**, 634-638 (2014). <http://dx.doi.org/10.1016/j.matdes.2013.07.067>.
- [6] S. Furuta, M. Kobayashi, K. Uesugi, A. Takeuchi, T. Aoba, H. Miura, Materials Characterization **130**, 237-242 (2017). <http://dx.doi.org/10.1016/j.matchar.2017.06.009>.
- [7] S. G. Krishna, International Journal on Theoretical and Applied Research in Mechanical Engineering **2**/1, 53-56 (2013).
- [8] R. Romankiewicz, F. Romankiewicz, Production Engineering Archives **3**/2, 6-9 (2014).
- [9] P. Skočovský, E. Tillová, J. Belan, Archives of Foundry Engineering **9**/2, 169-172 (2009).
- [10] M. Timpel, N. Wanderka, R. Schlesiger, T. Yamamoto, N. Lazarev, D. Isheim, G. Schmitz, S. Matsumura, J. Banhart, Acta Materialia **60**/9, 3920-3928 (2012). <https://doi.org/10.1016/j.actamat.2012.03.031>.
- [11] Z.W. Chen, C.Z. Ma, P. Chen, Transaction of Nonferrous Metals Society of China **22**, 42-46 (2012). DOI: 10.1016/S1003-6326(11)61137-0.
- [12] Y. P. Lim, J. B. Ooi, X. Wang, Archives of Foundry Engineering **11**/4, 77-82 (2011).
- [13] R. Francis, J. Sokolowski, Metalurgija – Journal of Metallurgy **14**/1, 3-15 (2008). UDC:669.715'782.018.11.001.573=20.
- [14] C. Qiu, S. Mial, X. Li, X. Xia, J. Ding, Y. Wang, W. Zhao, Materials and Design **114**, 563-571 (2017). <https://doi.org/10.1016/j.matdes.2016.10.061>.
- [15] G.K. Sigworth. International Journal of Metal Casting **8**, 19-40 (2008).
- [16] Modification and refinement of aluminium silicon alloys, available on-line (28.3.2018) at <http://www.totalmateria.com/Article85.htm>
- [17] Z. Chen, R. Zhang, Research and Development, China Foundry **7**/2, 149-152 (2010).
- [18] L. Hurtalová, E. Tillová, M. Chalupová, M. Farkašová, Production Engineering Archives **3**/2, 2-5 (2014).
- [19] M. Farkašová, E. Tillová, M. Chalupová, FME Transactions **41**/3, 210-215 (2013).
- [20] M. Karamouz, M. Azarbarmas, M. Emany, M. Alipour, Materials Science and Engineering A. **582**, 409-414 (2013). <https://doi.org/10.1016/j.msea.2013.05.088>.
- [21] S.S. Sreeja-Kumari, R.M. Pillai, K. Nogita, A.K. Dahle, B.C. Pai, Metallurgical and Materials Transactions A. **37 A**, 2581-2587 (2006). DOI: 10.1007/BF02586230.
- [22] W. Ding, T. Xia, W. Zhao, Y. Xu, Materials (Basel) **7**/2, 1188-1200 (2014). doi:10.3390/ma7021188.
- [23] N. Haghdadi, A. Zarei-Hanzaki, H.R. Abedi, D. Abou-Ras, M. Kawasaki, A.P. Zhilyaev, Materials Science and Engineering A. **651**, 269-279 (2016). <http://dx.doi.org/10.1016/j.msea.2015.10.066>.
- [24] H.A. Elhadari, H.A. Patel, D.L. Chen, W. Kasprzyk, Materials Science and Engineering A. **528**, 8128-8138 (2011). <https://doi.org/10.1016/j.msea.2011.07.018>.
- [25] M. Nowak, L. Bolzoni, N.H. Babu, Materials and Design **66**, 366-375 (2015). <http://dx.doi.org/10.1016/j.matdes.2014.08.066>.
- [26] M.G. Mueller, G. Žagar, A. Mortensen, Acta Materialia **143**, 67-76 (2018). <https://doi.org/10.1016/j.actamat.2017.09.058>.
- [27] M.G. Muller, M. Fornabio, G. Žagar, A. Mortensen, Acta Materialia **105**, 165-175 (2016). <http://dx.doi.org/10.1016/j.actamat.2015.12.006>.
- [28] L. Zeng, J. Sakamoto, A. Fujii, H. Noguchi, Engineering Fracture Mechanics **115**, 1-12 (2014). <http://dx.doi.org/10.1016/j.engfracmech.2013.11.016>.
- [29] A. Mahato, S. Xia, T. Perry, A. Sachdev, S.K. Biswas, Tribology International **43**, 381-387 (2010). doi:10.1016/j.triboint.2009.06.020.
- [30] X. Zheng, H. Cui, C.C. Engler-Pinto Jr., X. Su, W. Wen, Materials Science and Engineering A. **580**, 71-76 (2013). <http://dx.doi.org/10.1016/j.msea.2013.05.045>.
- [31] V.D. Le, F. Morel, D. Bellett, E. Pessard, N. Saintier, P. Osmond, Procedia Engineering. **133**, 562-575 (2015). doi: 10.1016/j.proeng.2015.12.630.
- [32] C. Limmaneevichitr, W. Eidhed, Materials Science and Engineering A. **349**, 197-206 (2003). [https://doi.org/10.1016/S0921-5093\(02\)00751-7](https://doi.org/10.1016/S0921-5093(02)00751-7).
- [33] R. Cook, Grain refinement of aluminium-silicon foundry alloys, London and Scandinavian Metallurgical co Limited, England, 1998.
- [34] S.A. Alkahtani, E.M. Elgallad, M.M. Tash, A.M. Samuel, F.H. Samuel, Materials **9**/1, 45-57 (2016).
- [35] S.Z. Lu, A. Hellawell, The mechanism of silicon modification in aluminium silicon alloys: impurity induced twinning, Metall. Trans. A **18**, 1721-1733 (1987).
- [36] E. Samuel, A.M. Samuel, H.W. Doty, S. Valtierra, F.H. Samuel, Int. J. Cast Met. Res. **27**, 107-114 (2014). <https://doi.org/10.1179/1743133613Y.0000000083>.